



## Measurement of the beam parameter variations in DELPHI with the VSAT

S. Almedhed<sup>1</sup>, F. Cossutti<sup>2</sup>, Ch. Jarlskog<sup>1</sup>, G. Jarlskog<sup>1</sup>, P. Jonsson<sup>1</sup>,  
P. Poropat<sup>2</sup>, G. Rinaudo<sup>3</sup>, E. Vallazza<sup>4</sup>

### Abstract

The beam parameter variations during 1994 data taking, obtained by the measurements of the Very Small Angle Tagger (VSAT) luminometer, are presented; a comparison with 1993 data is shown.

---

<sup>1</sup>Lund

<sup>2</sup>Trieste

<sup>3</sup>Torino

<sup>4</sup>CERN

# 1 Introduction

The Very Small Angle Tagger (VSAT) is an electromagnetic sampling calorimeter for the luminosity measurement in DELPHI. It consists of four rectangular modules placed symmetrically at about 7.7 m from the DELPHI origin, around a short elliptical section of the beam pipe behind the low beta superconducting quadrupoles (SCQ) as shown in fig. 1. The distance between two neighbouring modules is about 12 cm, corresponding to the smaller beam pipe dimension in that region. Since the physical process studied for the luminosity measurement is the Bhabha scattering, where electrons and positrons are emitted back to back, we use the coincidences of signals between a module in the forward region and a module in the backward region, thus defining two diagonals for the trigger: diagonal 1 (modules F1-B2) and diagonal 2 (modules F2-B1).

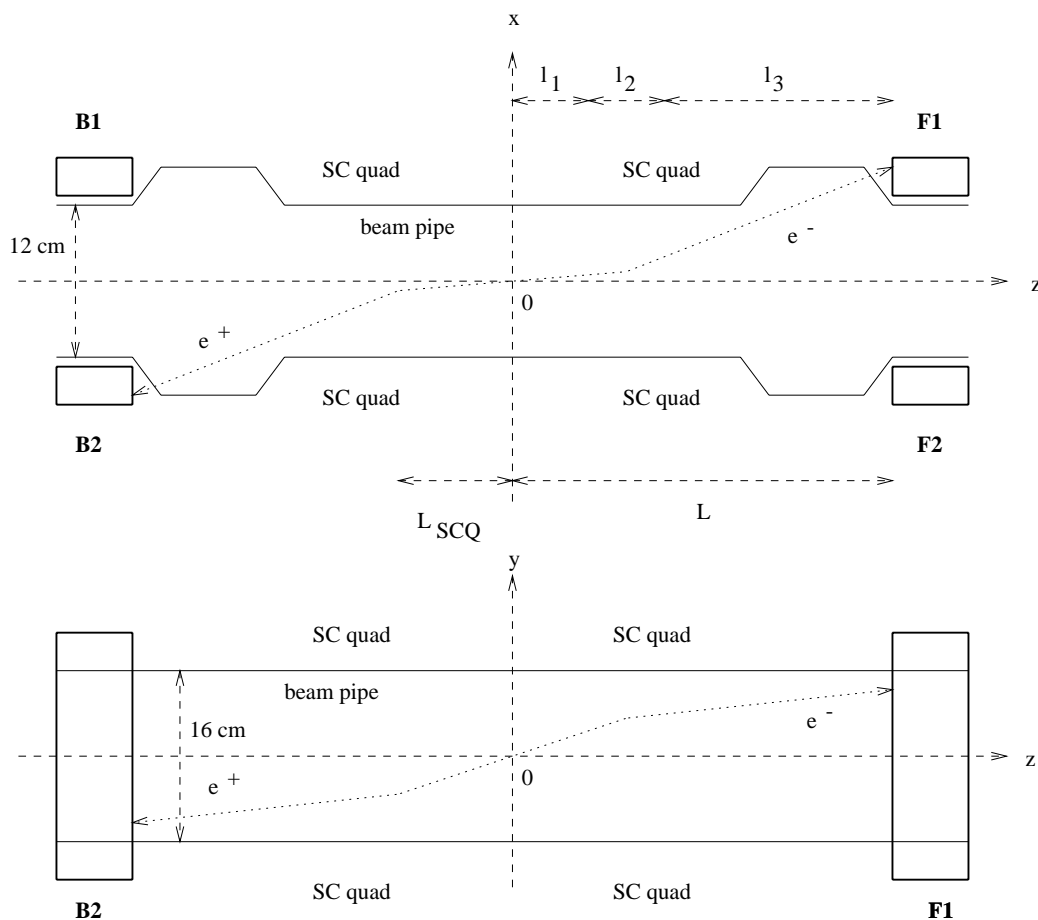


Figure 1: *Layout of the position of the VSAT modules in the  $(x, z)$  and  $(y, z)$  planes: the distance  $L_{SCQ}$  of the center of the superconducting quadrupoles from the DELPHI origin is about 4 m and the distance  $L$  of the front of the VSAT modules is about 7.7 m; the distances  $l_1$ ,  $l_2$  and  $l_3$  define the three regions relevant to the beamspot equations.*

Each VSAT module contains 12 tungsten absorbers ( $X_0 = 0.38$  cm) interspaced with 12 silicon planes (Full Area Detectors, (FAD)) for energy measurement (fig. 2). The

dimensions of the calorimeters are 3 cm in the transverse horizontal direction ( $x$ ), 5 cm in the vertical direction ( $y$ ) and 24 radiation lengths (about 10 cm) along the beam direction ( $z$ ). The center of the electromagnetic shower is given by three silicon strip planes with 1 mm pitch placed close to the shower maximum at 5, 7 and 9  $X_0$ ; the second plane is used for the  $y$  coordinate measurement and the other two planes for the  $x$  coordinate measurement. More details are given in references [1], [2], [3] and [4].

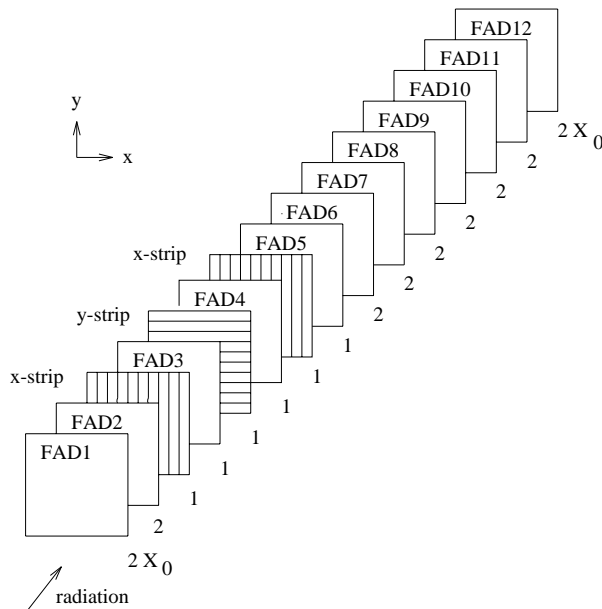


Figure 2: *Layout of the VSAT modules.*

Due to the very small emission angle of the Bhabha events accepted in the VSAT, in spite of the restricted angular acceptance of the detector (between 5 and 7 mrad in polar angle and about 50 degrees in azimuth), the accepted Bhabha cross section is very large (about 500 nb): this allows to monitor with high statistics, besides the luminosity, also the beam background and the variation of beam parameters.

The effect of the variation of beam parameters on the quantities measured by the VSAT will be discussed in section 2. In section 3, the procedure used to obtain the information on the beam parameters will be described and their variation during 1994 will be discussed.

## 2 Beam parameters monitoring with the VSAT

The beam parameters that are relevant for the following discussion are:

- the average values of the coordinates  $x_b$ ,  $y_b$  and  $z_b$  of the interaction point;
- the corresponding beam widths  $\sigma_x$ ,  $\sigma_y$  and  $\sigma_z$ ;
- the average values of the incident positron and electron beam directions at the interaction point, in the  $(x, z)$  and in the  $(y, z)$  planes (we will call them briefly *tilts*), respectively  $\theta_+^x$ ,  $\theta_-^x$ ,  $\theta_+^y$  and  $\theta_-^y$ ;

- the beam divergence in the two planes, that is the spread around the above average directions.

The quantities measured with the VSAT which are used to extract information on the beam parameters are the x and y coordinates of the impact points of the scattered leptons on the four modules, while their directions cannot be measured. In the following two sections, we will discuss the dependence on the beam parameters of such coordinates.

## 2.1 Beam parameters in the (x,z) plane

The transport of the positron and the electron from the interaction point to the VSAT module is given by the product of three matrices which describe the trajectory in the three relevant regions shown in fig. 1:

- region 1, of length  $l_1$ , from the interaction point to the superconducting quadrupole in the DELPHI solenoid;
- region 2, of length  $l_2$ , through the superconducting quadrupole;
- region 3, of length  $l_3$ , from the superconducting quadrupole to the VSAT module.

Since the effect of the DELPHI solenoid is completely negligible for the Bhabha electrons in the VSAT, trajectories in region 1, as well as 3, are straight lines and the resulting equations between initial and final coordinates and directions are linear. Explicitly, the x coordinates of the impact points on the four VSAT modules are:

$$\begin{aligned} x_{F1} &= f_x(x_b - z_b(\theta_1^x + \theta_-^x)) + l_x(\theta_1^x + \theta_-^x) & x_{B2} &= f_x(x_b - z_b(\theta_1^x + \theta_+^x)) - l_x(\theta_1^x + \theta_+^x) \\ x_{B1} &= f_x(x_b + z_b(\theta_2^x - \theta_+^x)) + l_x(\theta_2^x - \theta_+^x) & x_{F2} &= f_x(x_b + z_b(\theta_2^x - \theta_-^x)) - l_x(\theta_2^x - \theta_-^x) \end{aligned} \quad (1)$$

where  $x_b$ ,  $z_b$  are the x and z coordinates of the interaction point,  $\theta_1^x$  and  $\theta_2^x$  are the production angles in diagonal 1 and 2, respectively (always assumed to be positive) and  $\theta_+^x$  ( $\theta_-^x$ ) is the tilt angles in the (x,z) plane of the incident positron (electron). The coefficients  $f_x$  and  $l_x$  are functions of the lengths  $l_1$ ,  $l_2$  and  $l_3$  of the three regions and of the "k-factor" of the superconducting quadrupoles. For the values of 1993 and 1994 periods, their values are:

$$f_x = 2.1 \pm 0.1 \quad l_x = (12.60 \pm 0.02)m \quad (2)$$

essentially equal for the four modules. Eqs. (1) show that particle trajectories can be treated as straight lines by assuming the modules to be located at an effective distance,  $l_x$ , from the center of DELPHI ( $z_b=0$ ). Fig. 3 illustrates different situations, corresponding to one or more of the four beam parameters ( $x_b$ ,  $z_b$ ,  $\theta_+^x$ ,  $\theta_-^x$ ) being different from zero.

From eqs. (1), we see that it is convenient to use the quantities:

$$\begin{aligned} \Delta x_1 &= x_{F1} + x_{B2} = 2 \cdot f_x(x_b - z_b(\theta_1^x + \theta_x)) + \epsilon_x l_x \\ \Delta x_2 &= x_{F2} + x_{B1} = 2 \cdot f_x(x_b + z_b(\theta_2^x - \theta_x)) + \epsilon_x l_x \end{aligned} \quad (3)$$

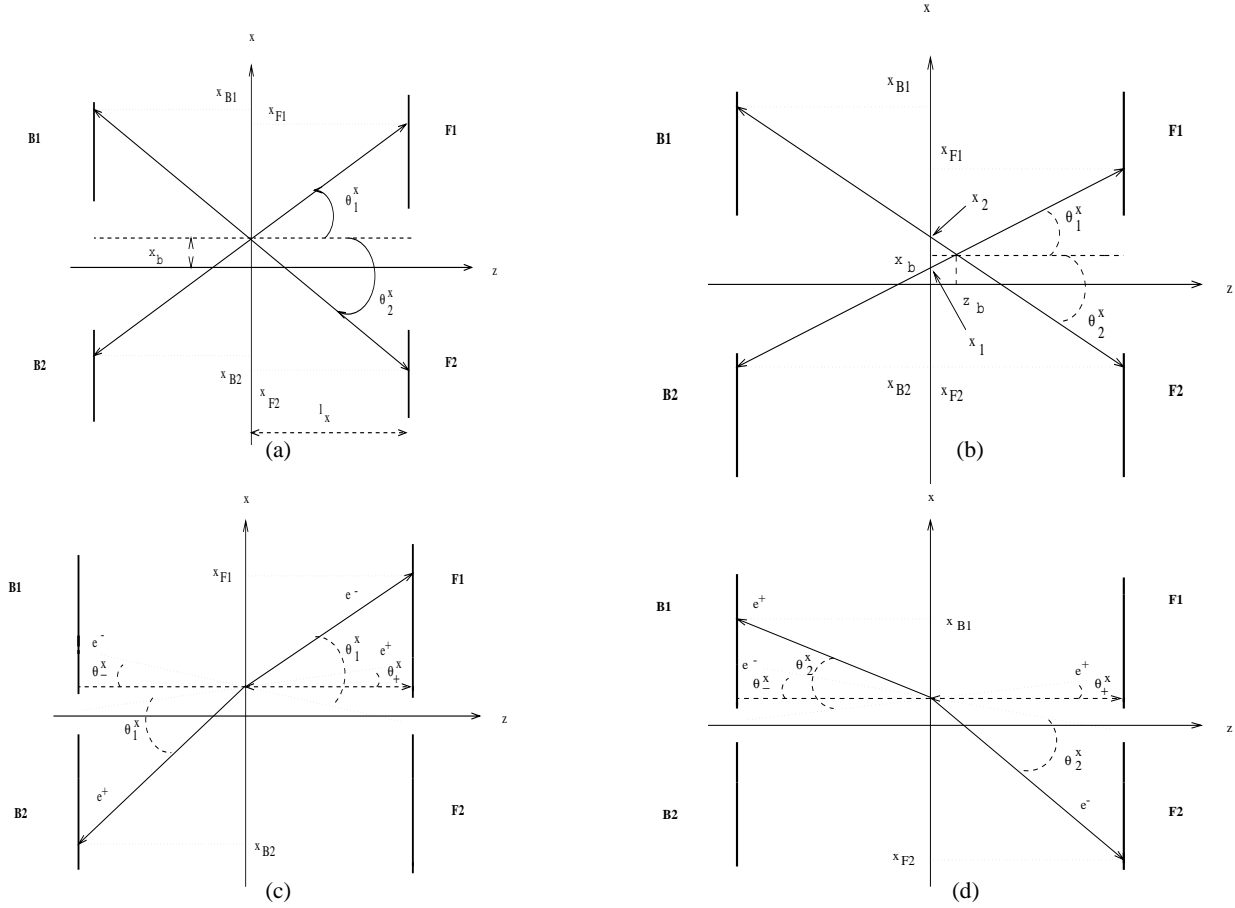


Figure 3: (a) events with positive  $x$  displacement, zero  $z$  displacement and zero tilts; (b) events with the same values of  $x$  displacement and tilts but with a positive displacement in  $z$ ; events for which only the  $z$  displacement is zero, in diagonal 1 (c) and in diagonal 2 (d).

where we have defined the average tilt,  $\theta_x$ , and the acollinearity,  $\epsilon_x$ , as follows

$$\theta_x = \frac{\theta_+^x + \theta_-^x}{2} \quad \epsilon_x = \theta_-^x - \theta_+^x \quad (4)$$

Eqs. (3) evidenciate the similarity of the  $x_b$  and  $\epsilon_x$  effects on the impact points. This is more clearly depicted in fig. 4, where we have assumed for simplicity that only the electron beam has a nonzero tilt: the full lines correspond to outgoing particle tracks for  $x_b = \theta_-^x = \theta_+^x = 0$ , whereas the dotted line shows the case of nonzero acollinearity and  $x_b=0$  and the dashed line shows an event with zero acollinearity but nonzero  $x_b$ , which has the same impact points on the modules, showing that the  $\epsilon_x$  and  $x_b$  effects are equivalent, and therefore these two parameters cannot be determined separately using the VSAT information alone.

To better separate the dependence on different beam parameters, we define the following quantities:

$$\Delta x = \frac{\Delta x_1 + \Delta x_2}{2} = 2 \cdot f_x x_b + \epsilon_x l_x + f_x z_b (\theta_2^x - \theta_1^x - 2\theta_x) \quad (5)$$

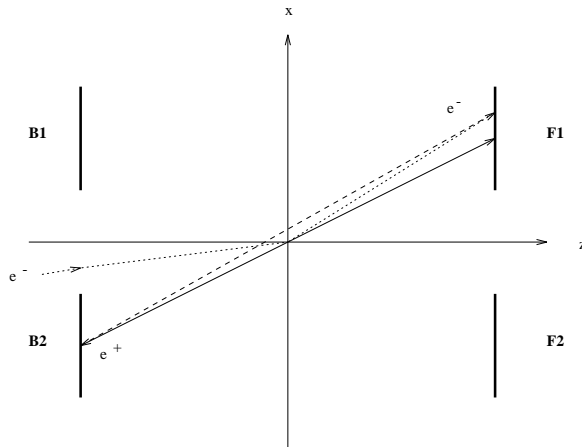


Figure 4: *Effects of the acollinearity and the  $x$  displacement on the impact points.*

$$\delta x = \Delta x_2 - \Delta x_1 = 2 \cdot f_x z_b (\theta_1^x + \theta_2^x) \quad (6)$$

By taking the average over a reasonably long period of time (we usually assume the time needed to write a cassette, which is about 20 minutes and corresponds to about 4 K events), we can substitute to  $\theta_1^x$  and  $\theta_2^x$  their average values,  $\overline{\theta_i^x}$ , which are both very close to 5.5 mrad. The equations show that the average value of the  $\delta x$  distribution essentially depends only on the value of  $z_b$ . On the contrary, the average value of the  $\Delta x$  distribution essentially measures the combined effect of the beam  $x$  displacement and beam acollinearity in the  $(x,z)$  plane, since the third term in eq. (5) is completely negligible.

From eq. (5) it also follows that the dispersion  $\sigma_{\Delta x}$  of the  $\Delta x$  distribution is related to the dispersion of the distribution of  $x_b$  and  $\epsilon_x$ , i.e. to the beam parameters  $\sigma_x$  and  $\sigma_{\theta_x}$ :

$$\sigma_{\Delta x} = 2 f_x \sigma_x + l_x \sigma_{\theta_x} + \sigma_m \quad (7)$$

where  $\sigma_m$  is the measurement error on  $\Delta x$ . The first and the third term are small compared to the middle one and are also rather well known, thus  $\sigma_{\Delta x}$  can be used to measure the beam divergence,  $\sigma_{\theta_x}$ .

However, due to the limited VSAT acceptance, the averaging procedure introduces second order dependences on the beam parameters, which can only be evaluated by an appropriate Monte Carlo simulation. We used to this aim the extensive simulations of different beam conditions which were done with the fast simulation program FASTSIM to determine the VSAT acceptance of Bhabha events for the measure of the luminosity (details of the program are found in [2]). Two major dependences are found: on  $\sigma_x$  and  $\sigma_{\theta_x}$ , i.e. on the widths of the  $x_b$  and  $\epsilon_x$  distributions and on the  $y$  tilt. Fortunately, both such dependences can be parametrized in terms of quantities directly measured by the VSAT, the former by  $\sigma_{\Delta x}$  and the latter by the quantity  $\Delta y$ , which will be introduced below. The resulting corrections to  $\Delta x$  and  $\delta x$  are small and linear. Also, all the effective parameters of eq. (5) and (6), such as  $f_x$  and  $l_x$ , have been calculated with FASTSIM.

There are two other useful measures that can be done with the VSAT and which are related to the beam tilts. With a view to this, it is helpful to consider events with equal

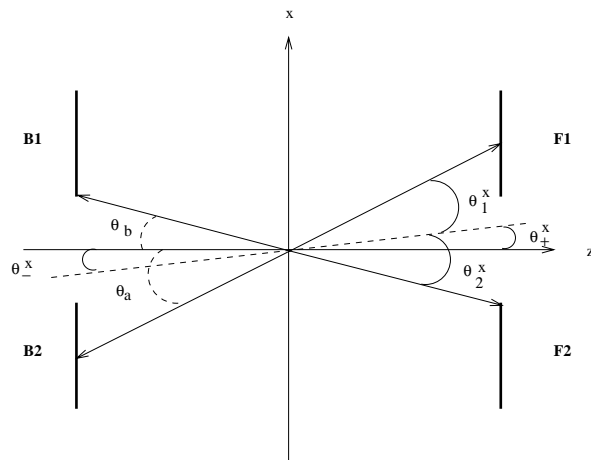


Figure 5: *Effect of the beam tilts on the production angles on the two diagonals.*

(positive) beam tilt angles,  $\theta_+^x$  and  $\theta_-^x$ , as in fig. 5. The figure shows clearly that for the same values of the impact points the production angle on diagonal 1,  $\theta_1^x$ , is smaller than in the case of zero tilts, where it would be equal to  $\theta_a$ , while the opposite holds for the production angle on diagonal 2 ( $\theta_2^x$  is larger than  $\theta_b$ ). Due to the rapid decrease of the Bhabha cross section with the angle, this induces an opposite variation of the number of accepted Bhabha events on the two diagonals: the number of events on diagonal 1,  $N_1$ , will increase, whereas the number of events on diagonal 2,  $N_2$ , will decrease. Therefore, we expect to observe a variation of the variable:

$$A_D = \frac{N_1 - N_2}{N_1 + N_2} \quad (8)$$

called *diagonal asymmetry*. It must be noted, however, that the diagonal asymmetry is only affected by the average tilt angle,  $\theta_x$ , and not by the separate values of  $\theta_-^x$  and  $\theta_+^x$ . By consequence, it cannot be used to extract information on the acollinearity,  $\epsilon_x$ . The relationship between  $A_D$  and  $\theta_x$  has been evaluated by FASTSIM.

## 2.2 Beam parameters in the (y,z) plane

The transport equations in the (y,z) plane are very similar to those of the (x,z) plane:

$$\begin{aligned} y_{F1} &= f_y(y_b - z_b(\theta_1^y + \theta_-^y)) + l_y(\theta_1^y + \theta_-^y) & y_{B2} &= f_y(y_b - z_b(\theta_1^y + \theta_+^y)) - l_y(\theta_1^y + \theta_+^y) \\ y_{B1} &= f_y(y_b + z_b(\theta_2^y - \theta_+^y)) + l_y(\theta_2^y - \theta_+^y) & y_{F2} &= f_y(y_b + z_b(\theta_2^y - \theta_-^y)) - l_y(\theta_2^y - \theta_-^y) \end{aligned} \quad (9)$$

There are however two important differences with respect to the (x,z) plane. The first difference is due to the fact that in the y direction the superconducting quadrupoles have a convergent effect, opposed to the divergent effect in the other plane. This gives values for the  $f_y$  and  $l_y$  parameters which are much smaller than those of the corresponding parameters in the (x,z) plane:

$$f_y = 0.10 \pm 0.02 \quad l_y = (3.50 \pm 0.02)m \quad (10)$$

In particular, because of the small value of  $f_y$ , VSAT measures in the (y,z) plane are practically insensitive to the values of  $y_b$  and  $z_b$ . The second difference is the small angle of the production angles  $\theta_1^y$  and  $\theta_2^y$ , which average to zero.

We define

$$\Delta y_1 = y_{F1} + y_{B2} \quad \Delta y_2 = y_{F2} + y_{B1} \quad (11)$$

and

$$\Delta y = \frac{\Delta y_1 + \Delta y_2}{2} \quad (12)$$

Taking the average value over one cassette, we obtain

$$\Delta y = 2f_y y_b + l_y \epsilon_y \quad (13)$$

where we have defined the average acollinearity,  $\epsilon_y$ , in a similar way as for the (x,z) plane.

Information on the average tilt

$$\theta_y = \frac{\theta_+^y + \theta_-^y}{2} \quad (14)$$

is provided by the difference

$$y_{F1} - y_{B2} \approx y_{F2} - y_{B1} \approx 2 l_y \theta_y \quad (15)$$

We point out that a similar measure is in principle possible also in the (x,z) plane to obtain the value of  $\theta_x$ , however, due to the narrow acceptance of the VSAT calorimeters, fluctuations in the average production angle completely mask possible effects of  $\theta_x$ : for this reason in the (x,z) plane we use the diagonal asymmetry,  $A_D$ , which provides a much better measure of  $\theta_x$ .

Finally, the width,  $\sigma_{\Delta y}$ , of the  $\Delta y$  distribution can be used to obtain the y divergence,  $\sigma_{\theta_y}$ , of the beams.

### 3 Variation of the beam parameters

From VSAT data alone we can estimate the z coordinate of the interaction point using eq. (6), but this is not possible neither for the x nor for the y coordinate. This is due to the fact that, as shown in eq. (5) and (13), the detector variables depend both on the beam displacement and on the acollinearity in those directions. However, we can use eqs. (5) and (13) together with the beamspot values for x and y as they are determined by VD and TPC to obtain information on the variations of acollinearity.

#### 3.1 Estimation of z beamspot

From eq. (6), we have

$$z_b = \frac{\delta x}{2f_x(\theta_1^x + \theta_2^x)} \quad (16)$$

where  $\delta x$  has been corrected for second order dependence on beam parameters as explained in section 2. The sum of the production angles can be derived from the expressions of the impact points, eq. (1), as follows:

$$\theta_1^x + \theta_2^x = \frac{x_{F1} - x_{B2} - x_{F2} + x_{B1}}{2 \cdot l_x} \quad (17)$$



The distribution of  $z_b$  during 1994 is given in fig. 6. We observe an increase by 3 mm during period 1, a decrease of 1 mm during period 3 and small variations in period 2.

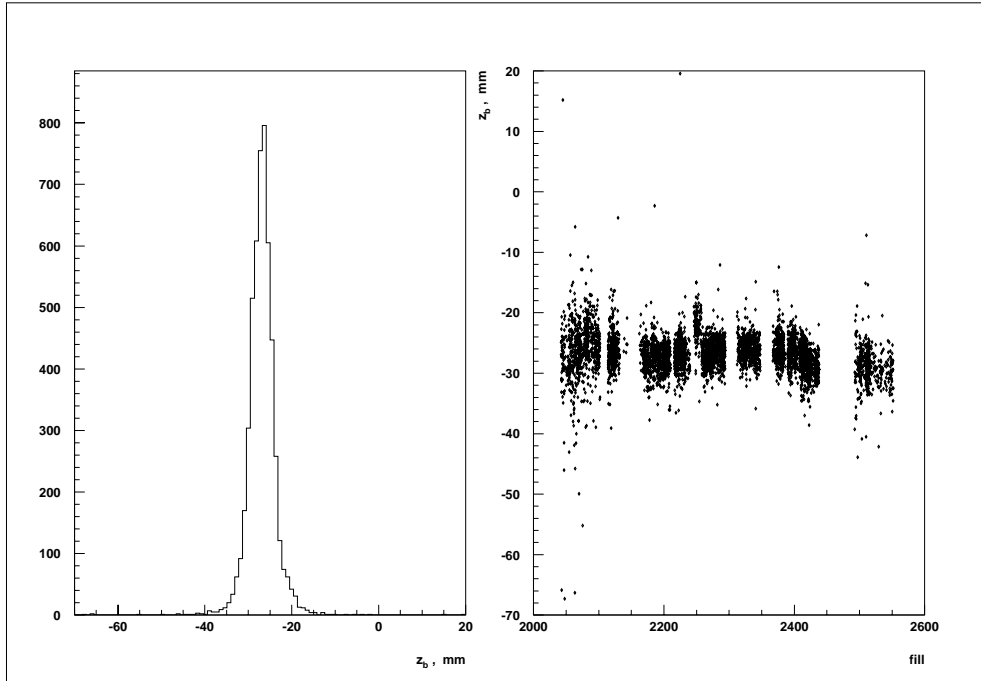


Figure 6:  $z$  beamspot from  $\Delta x_1$  and  $\Delta x_2$ .

In fig. 7, we have plotted the VSAT versus the TPC measurement for the  $z$  beamspot.

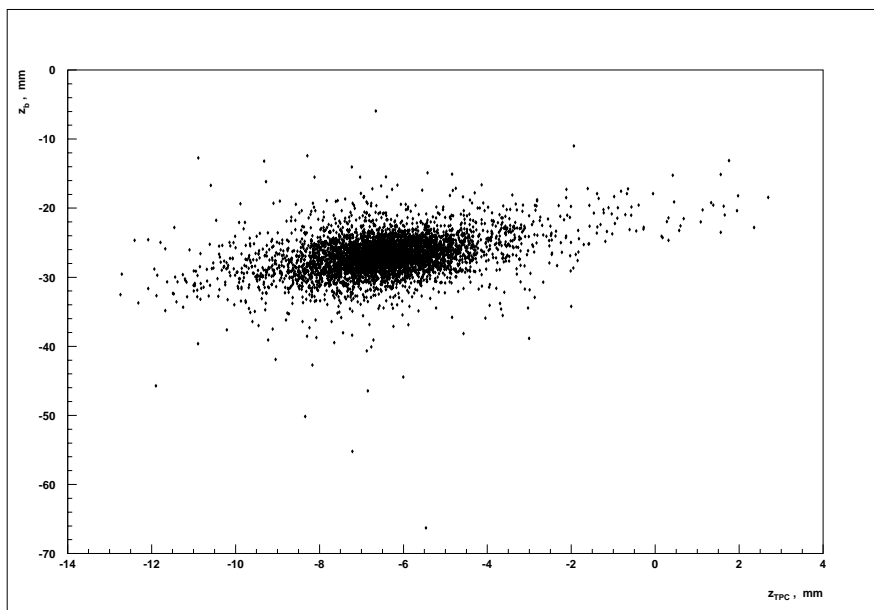


Figure 7:  $z_b$  from VSAT versus  $z_{TPC}$ .

In spite of the much larger error in the VSAT determination, We discern a linear relation, which is seen more clearly in the profile plot of fig. 8. The offset between the two measurements is of the order of 20 mm.

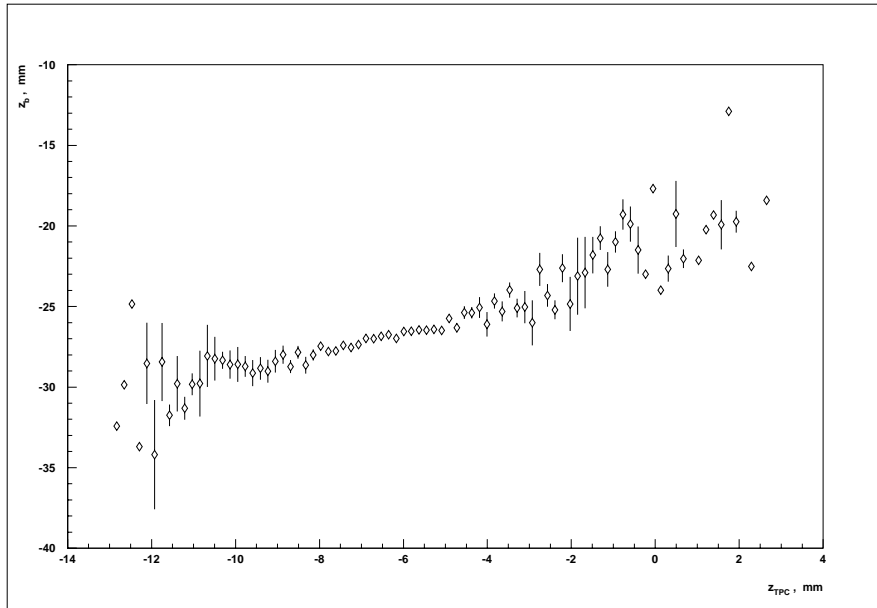


Figure 8: *Correlation between  $z_b$  and  $z_{TPC}$ , 1994 data.*

The distributions of the pulls of the VSAT and TPC determinations for all 1994 data and for the three periods are given in fig. 9 and 10, respectively and show that our

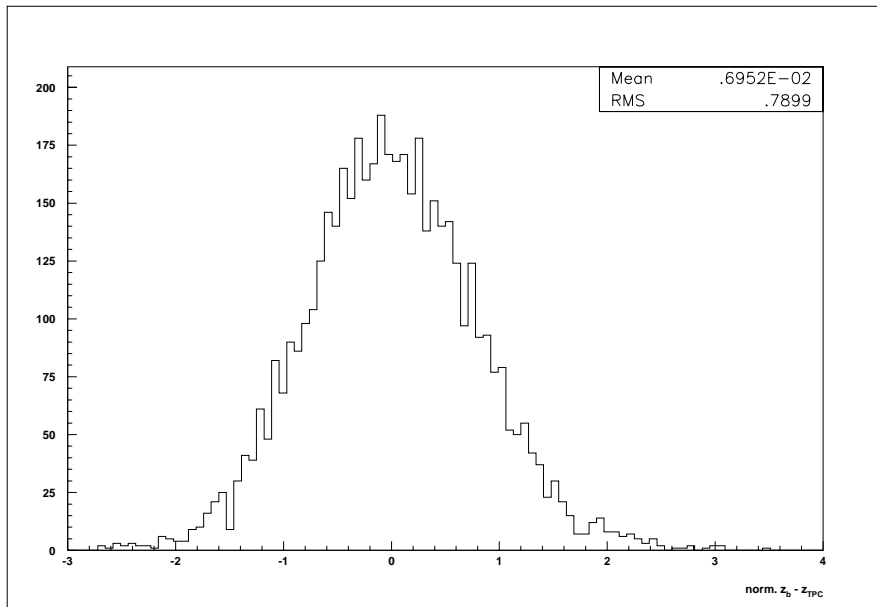


Figure 9: *Normalized difference between  $z_b$  and  $z_{TPC}$  for all 1994 data.*

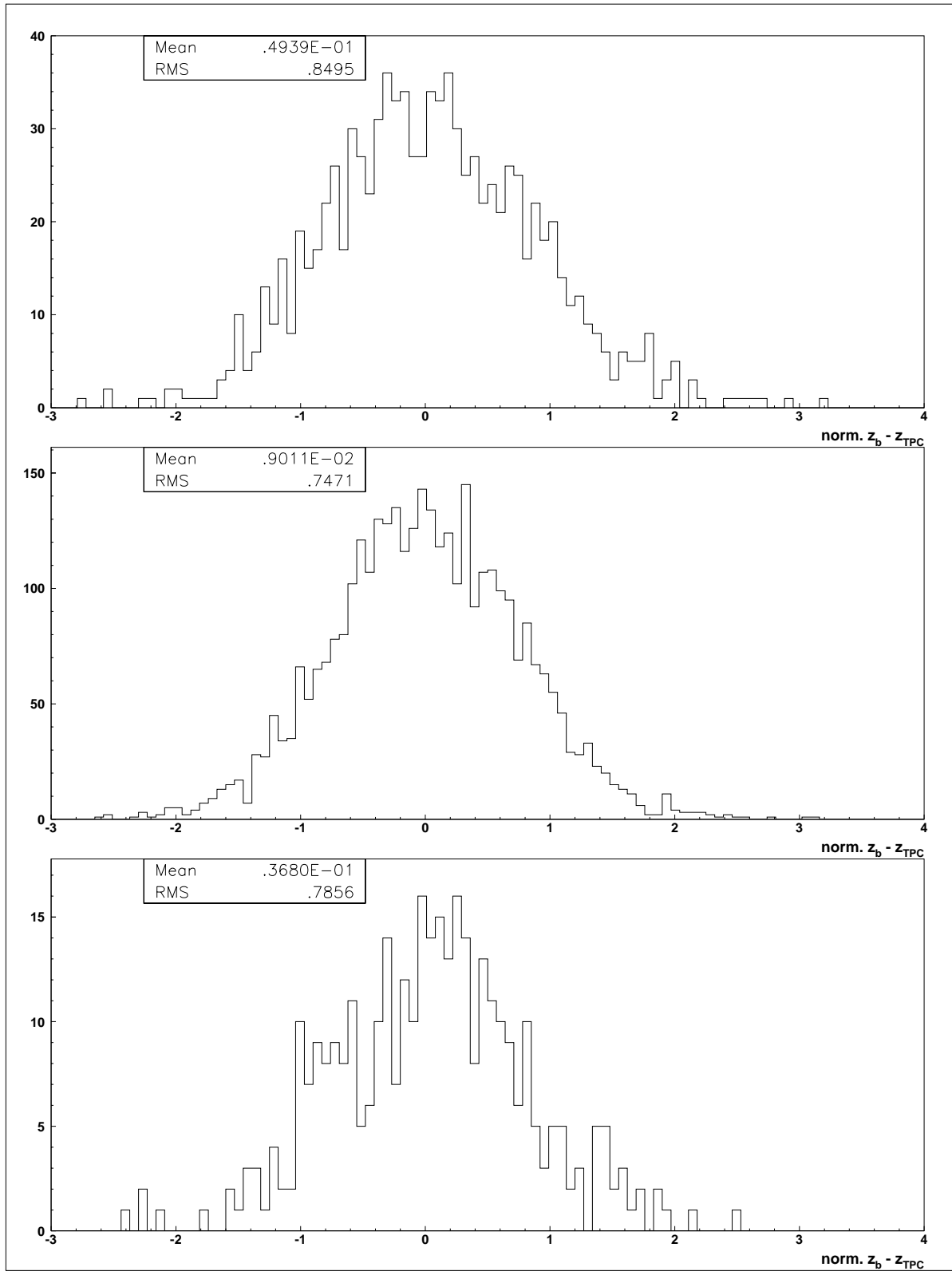


Figure 10: Normalized difference between  $z_b$  and  $z_{TPC}$ , 1994 data, periods 1, 2 and 3.

determination of  $z_b$  is compatible within errors with the TPC measure. The distributions of  $z_b$  for 1993 data and the corresponding difference from TPC are shown in figs. 11 and 12.

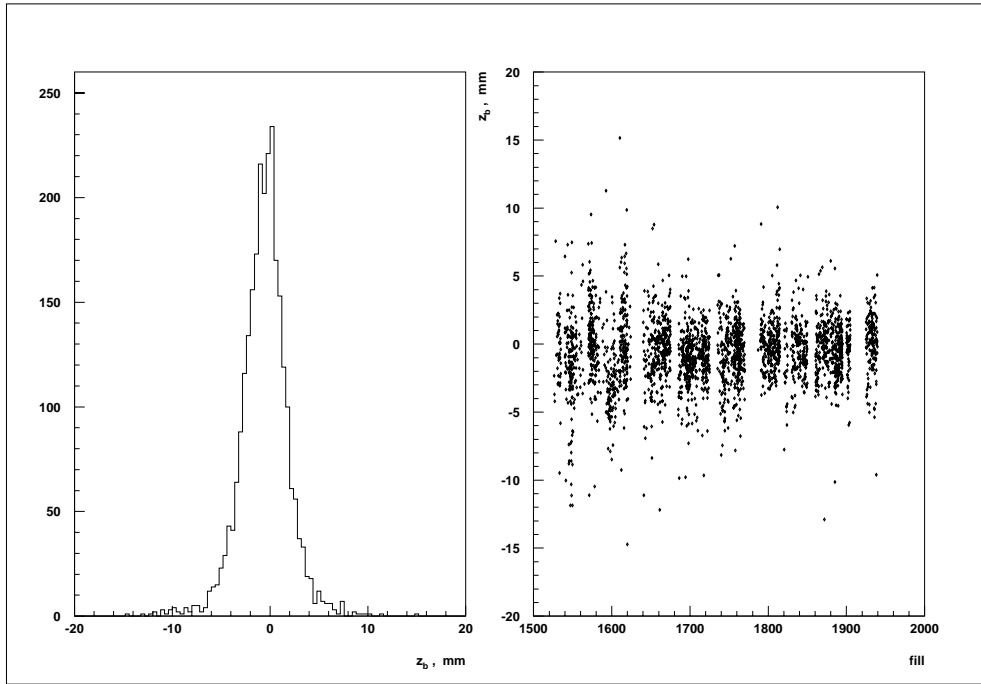


Figure 11:  $z_b$  from 1993 data.

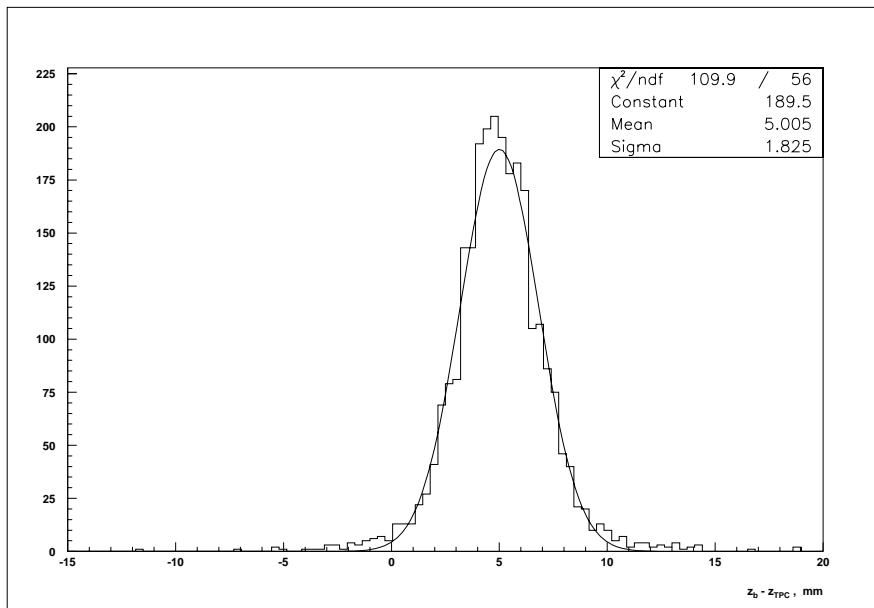


Figure 12: Difference between  $z_b$  and  $z_{TPC}$ , 1993 data.

### 3.2 Beam divergence, asymmetry and tilt

The variations of the beam width and divergence values are detected in terms of variations of  $\sigma_{\Delta x}$ . We show the variations of this parameter for 1994 in fig. 13.

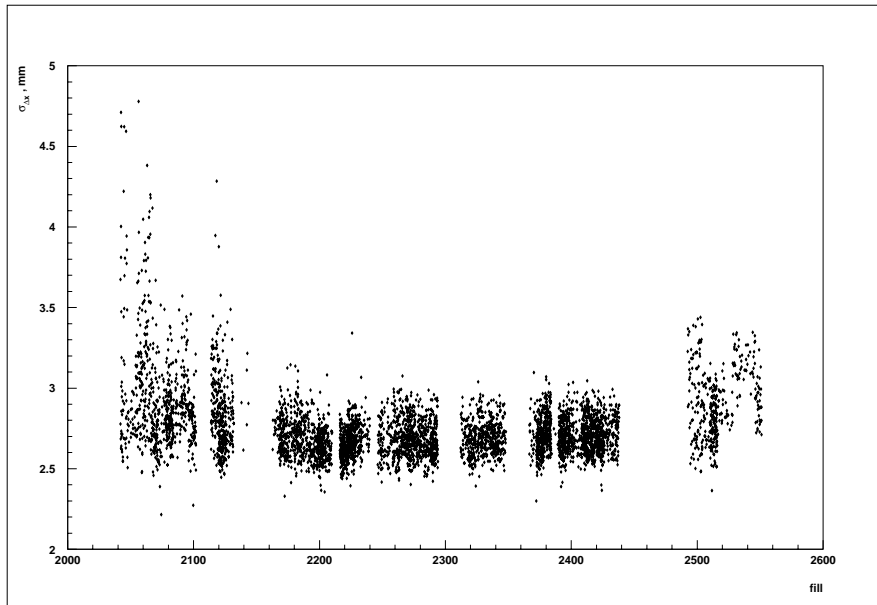


Figure 13: *Variation of  $\sigma_{\Delta x}$  during 1994.*

We see that  $\sigma_{\Delta x}$  varied from 2.2 mm to 4.8 mm in period 1, 3.4 mm in period 2 and 3.5 mm in period 3. There is an increase of the order of 50  $\mu\text{m}$  during period 2. This variable covered a smaller interval in 1993 than in 1994, i.e. from 2.4 mm to 3.4 mm, within which it manifested more moderate fluctuation than in the following year.

The variations of the tilt angle in the (x,z) plane are monitored by the diagonal asymmetry defined in eq. (8). They are shown in fig. 14 for 1994 data and in fig. 15 for 1993 data.

The mean tilt,  $\theta_y$ , in the (y,z) plane is monitored by the average y values of the impact points (see eq. 15). The variation of the mean tilt in the (y,z) plane during 1994 is given in fig. 16 and in fig. 17 for 1993 data.

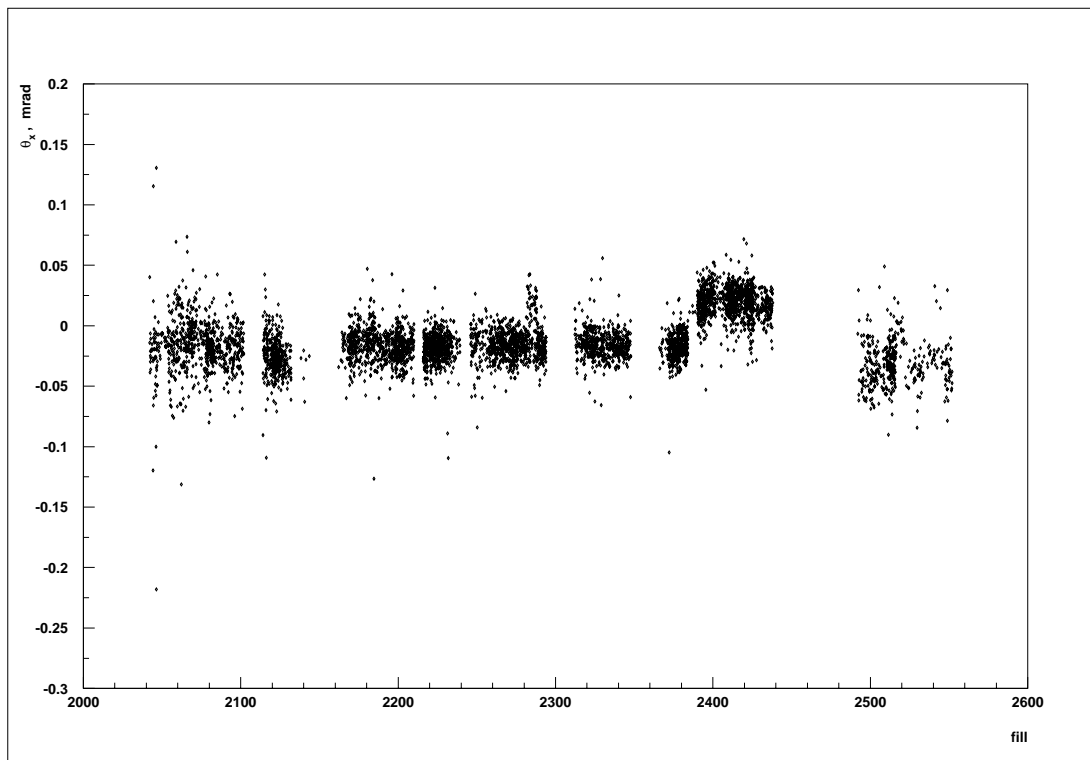


Figure 14: *Variation of  $\theta_x$  during 1994.*

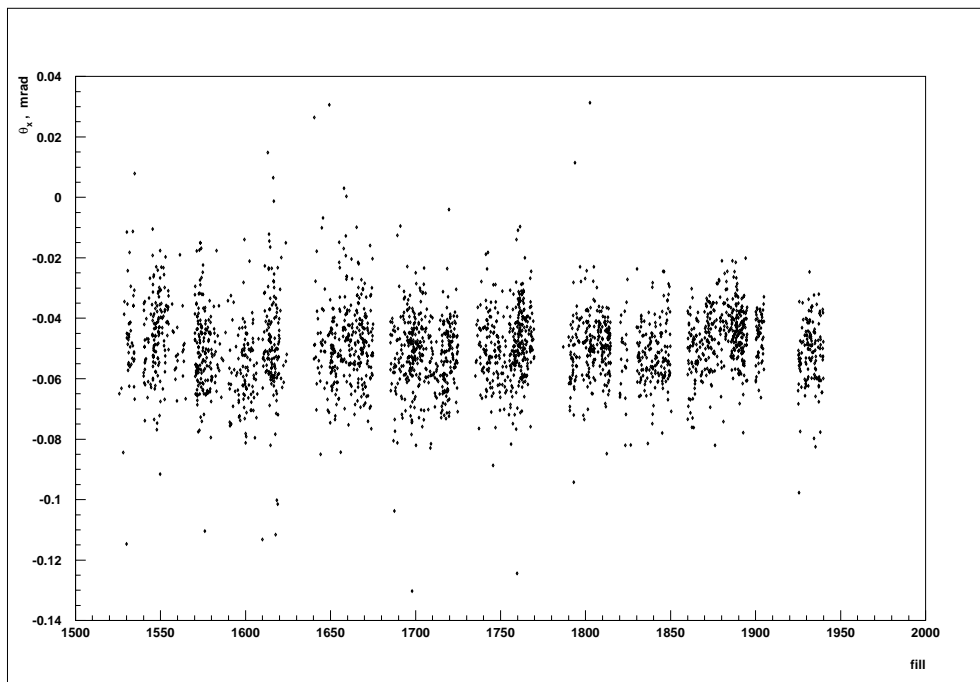


Figure 15: *Variation of  $\theta_x$  during 1993.*

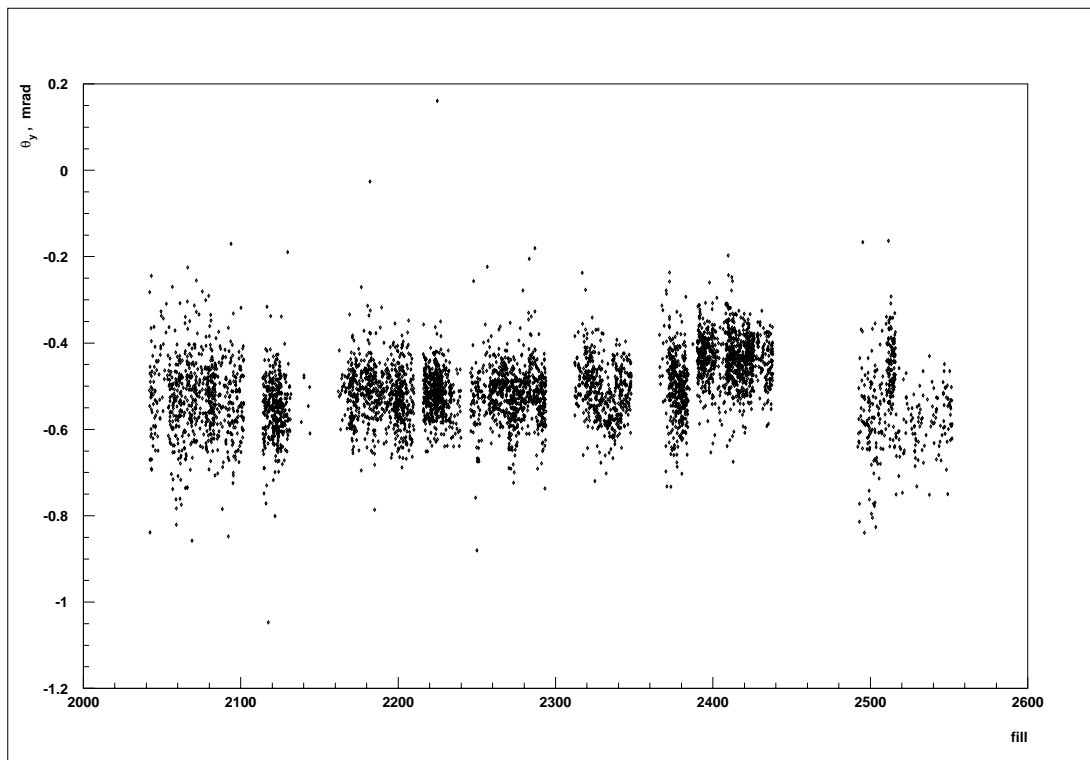


Figure 16: *Variation of  $\theta_y$  during 1994.*

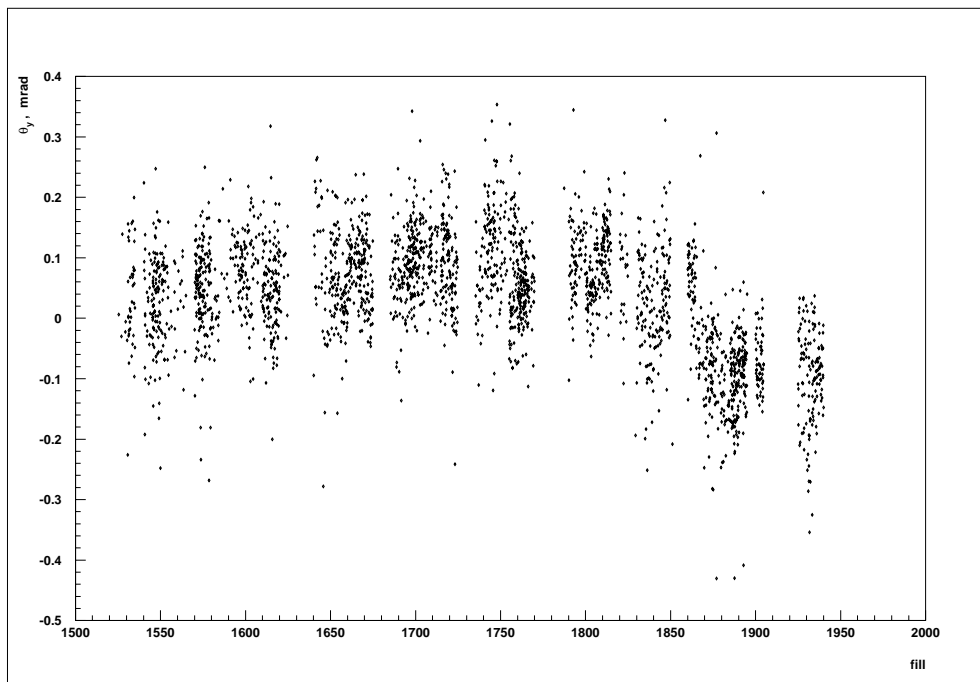


Figure 17: *Variation of  $\theta_y$  during 1993.*

### 3.3 Acollinearity

In order to obtain acollinearity estimations in the (x,z) and (y,z) planes, we introduce the VD values for  $x$  beamspot and  $y$  beamspot in eqs. (5) and (13), from which we obtain the following expressions:

$$\epsilon_x \approx \frac{\Delta x - 2f_x \cdot x_{VD}}{l_x} \quad (18)$$

and

$$\epsilon_y \approx \frac{\Delta y - 2f_y \cdot y_{VD}}{l_y} \quad (19)$$

Fig. 18 shows  $\epsilon_x$  for 1994 data. The most significant features are the increase of  $\epsilon_x$  of the order of 50  $\mu\text{rad}$  in period 1 and the rather large fluctuations in period 3. In fig. 19, the  $\epsilon_x$  data for 1993 are shown: the range of  $\epsilon_x$  fluctuations in 1993 was clearly smaller than in 1994.

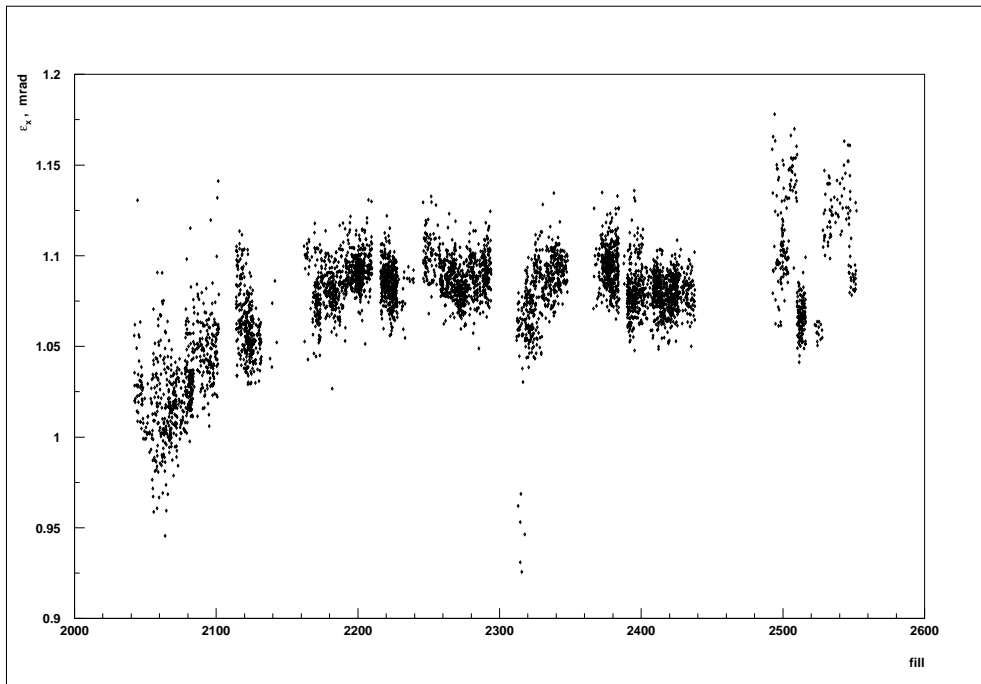


Figure 18: *Variation of  $\epsilon_x$  during 1994.*

The 1994 variations of the acollinearity in the (y,z) plane are shown in fig. 20. The variations are much larger than those of  $\epsilon_x$  with a large step of about 0.4 mrad between period 2 and periods 1 and 3. The  $\epsilon_y$  variations in 1993 data are shown in fig. 21, where no sharp variation is observed.

In figs. 22-25, we give the corresponding distributions of figs. 18-21 for the results presented by LEP. Apart from an overall shift of the mean values, the agreement between the VSAT and LEP determination of the acollinearity in both planes and during both years is very good.



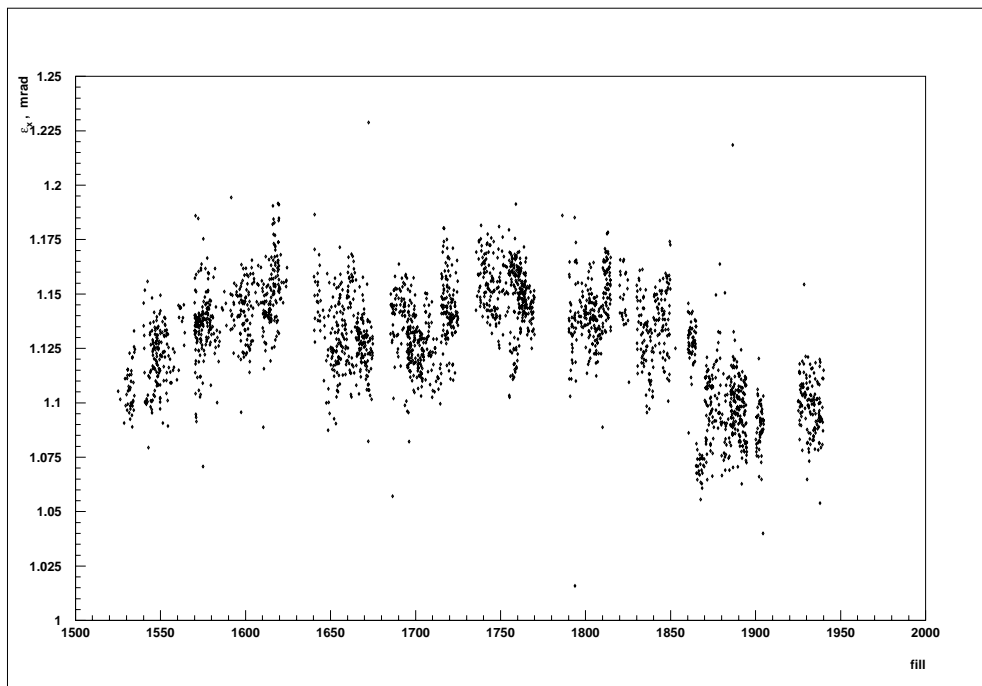


Figure 19: Variation of  $\epsilon_x$  during 1993.

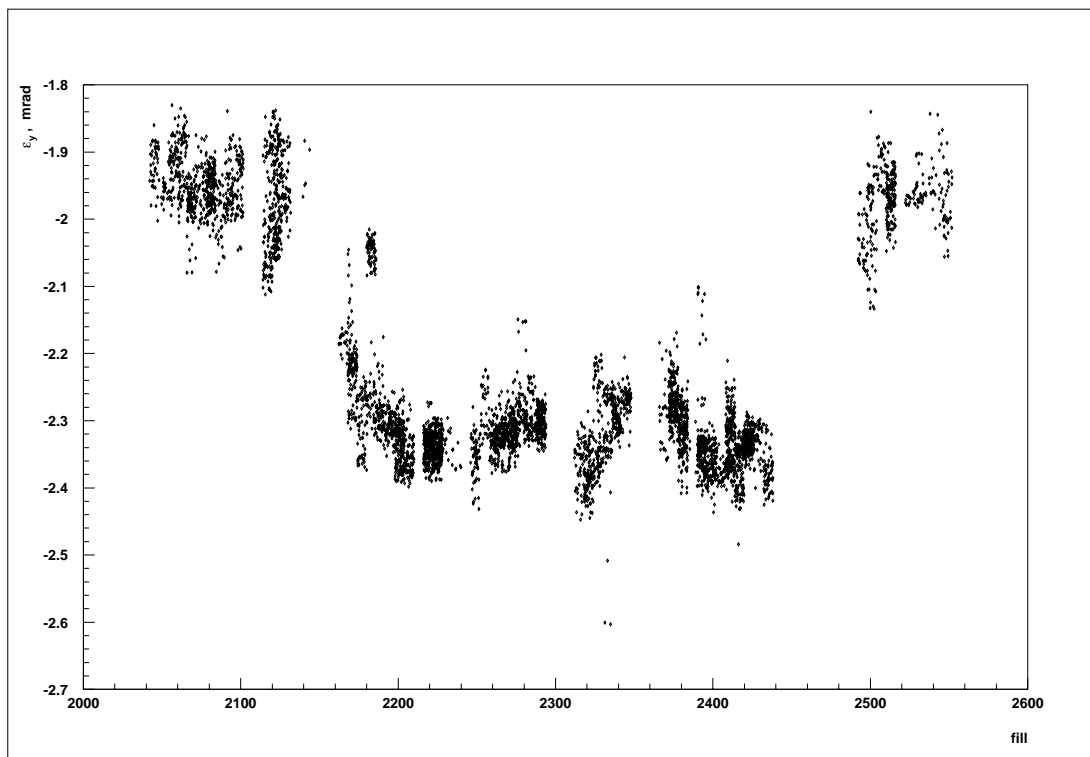


Figure 20: Variation of  $\epsilon_y$  during 1994.

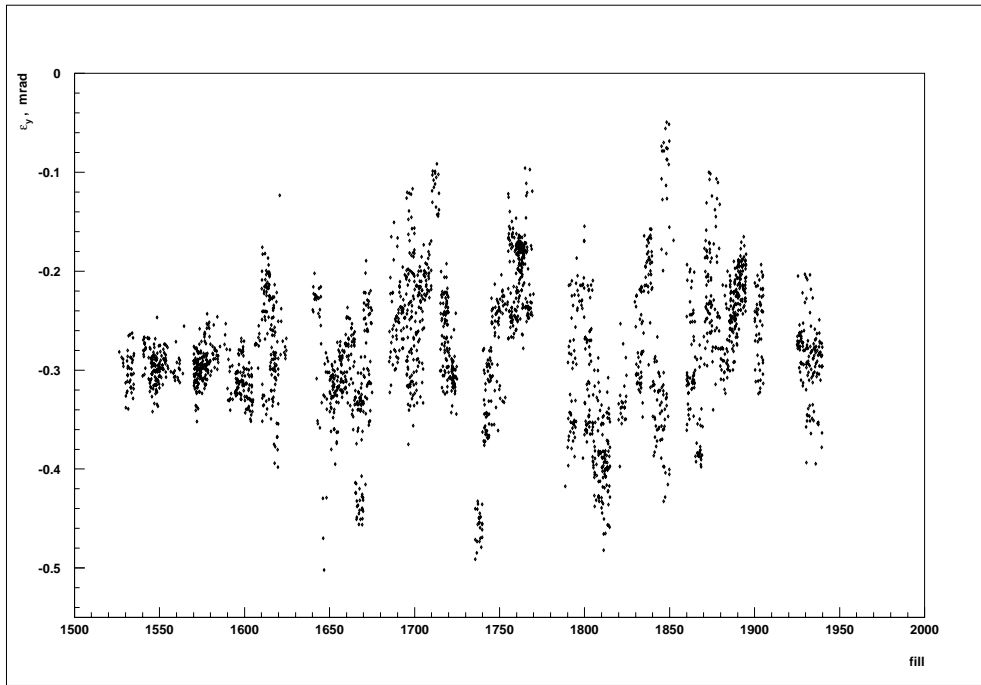


Figure 21: Variation of  $\epsilon_y$  during 1993.

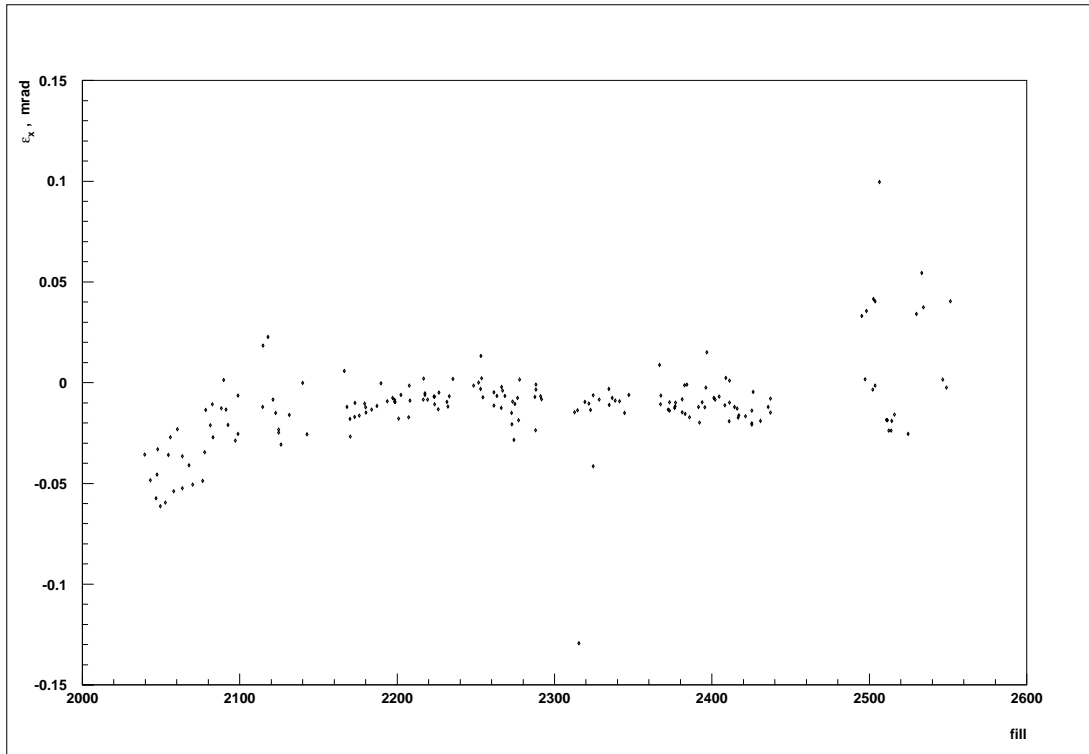


Figure 22:  $\epsilon_x$  from LEP during 1994.

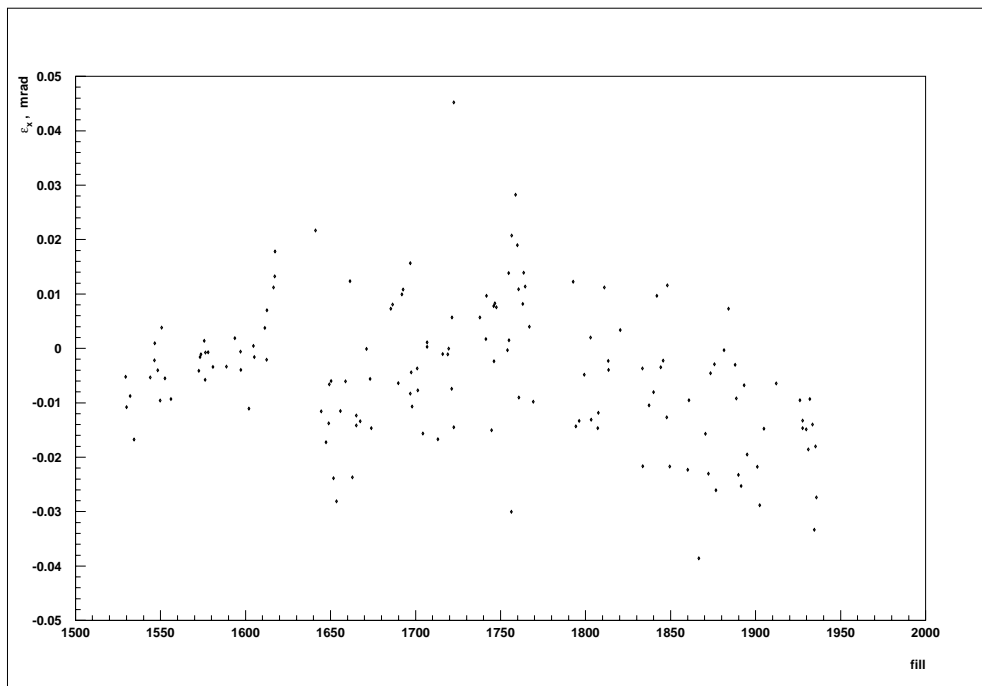


Figure 23:  $\epsilon_x$  from LEP during 1993.

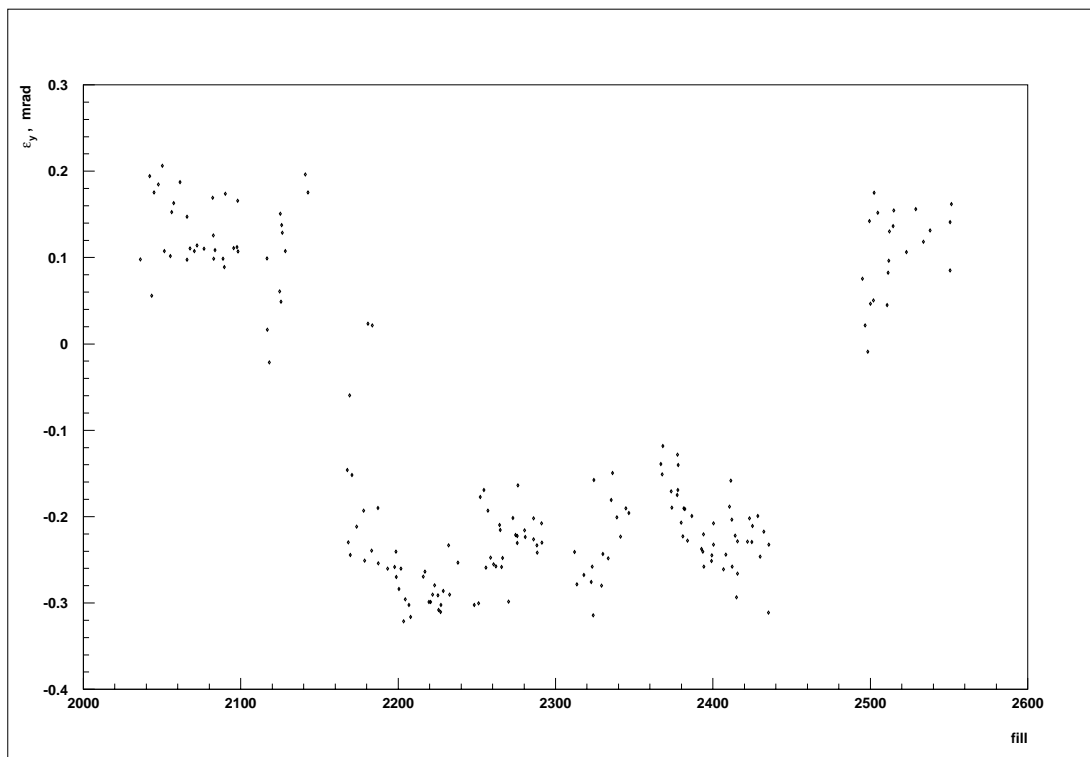


Figure 24:  $\epsilon_y$  from LEP during 1994.

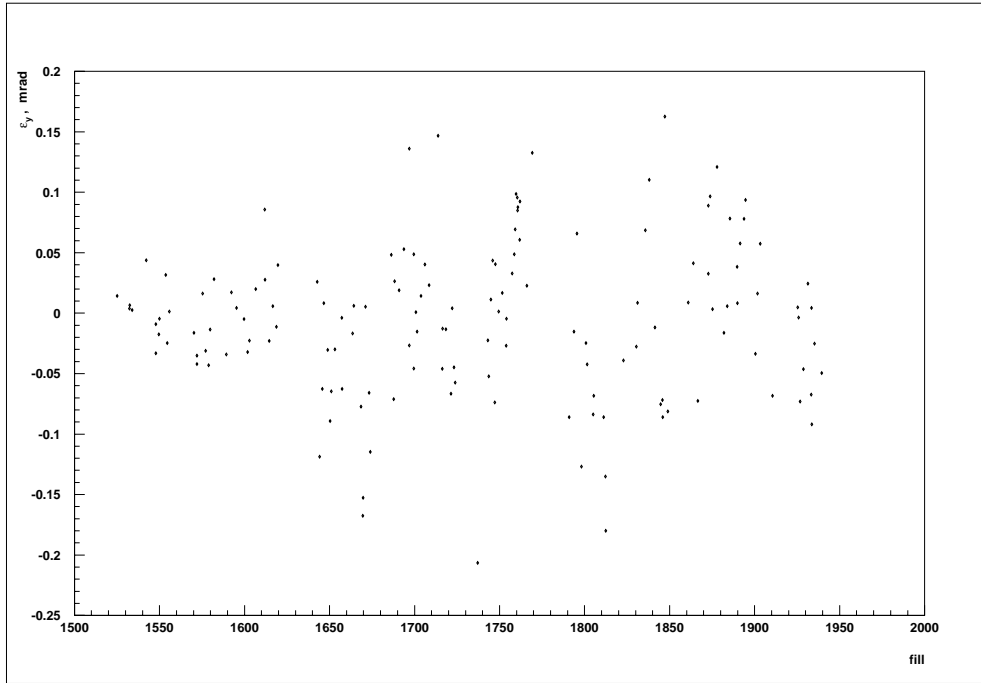


Figure 25:  $\epsilon_y$  from LEP during 1993.

## 4 Conclusions

The position of the VSAT allows for high accuracy measurements of variation in time of LEP beam parameters. In particular, we have shown that the VSAT measurements, combined with the measurements of the beam spot done by TPC and VD, give useful information on tilt and acollinearity of beams. This information cannot be obtained easily from other detectors in DELPHI and it is very useful for a better understanding of the beam conditions at the DELPHI interaction point, which are relevant for many physics analyses.

## References

- [1] Almehed et al., *A silicon tungsten electromagnetic calorimeter for LEP*.
- [2] Almehed et al., *High precision relative luminosity measurement with a Very Small Angle Tagger (VSAT) in DELPHI*, DELPHI 92-77 PHYS 188
- [3] Almehed et al., *Beam parameter monitoring and interaction point measurement in DELPHI with the VSAT* DELPHI 94-144 PHYS 453
- [4] Ch. Jarlskog, *Interaction point estimation and beam parameter variations in DELPHI with the VSAT*, LUNF D6/(NFFL-7110)/1995